Colloid Polym Sci (2005) 283: 551–558
DOI 10.1007/s00396-004-1185-1

ORIGINAL CONTRIBUTION

Keita Suzuki
Jun-ichi Oku
Kenichi Izawa
Hiro-Fumi Okabayashi
Isao Noda
Charmian J. O'Connor

Two-dimensional gel permeation chromatography (2D GPC) correlation studies of the aggregate-aggregate interactions in acid-catalyzed triethoxysilyl-terminated polystyrene systems. The effect of specific catalysts on growth process

Published online: 17 August 2004

K. Suzuki · J. Oku · H.-F. Okabayashi (✉)
Department of Applied Chemistry,
Nagoya Institute of Technology,
Gokiso-cho, 466-8555 Showa-ku,
Nagoya, Aichi, Japan
E-mail: fwiw4348@mb.infoweb.ne.jp

K. Izawa
Chromato Dept., Fuji Silysia Chemical
Ltd., 1846 Kozoji 2,
487-0013 Kasugai, Aichi, Japan

I. Noda
The Procter and Gamble Company,
8611 Beckett Road, West Chester,
OH 45069, USA

C. J. O'Connor
Department of Chemistry,
The University of Auckland,
Private Bag 92019, Auckland,
New Zealand

Abstract A set of time resolved gel-permeation chromatography (GPC) profiles, for the reaction mixture of a well-defined polymeric silane coupling agent, triethoxysilyl-terminated polystyrene with molecular weight equal to 8000 (TESi-PS (8000)), catalyzed by HCl (0.1 mol/kg) in tetrahydrofuran (THF), was measured over a long time scale (1–768 h). The GPC profiles were then converted to two-dimensional (2D) correlation spectra. The 2D GPC correlation spectra were compared with those for the CH_3SO_3H (0.1 mol/kg)-catalyzed TESi-PS (8000)-THF system. It has been demonstrated that predominant production of less-reactive oligomers in the HCl-catalyzed system hinders further growth of the oligomer, while formation of reactive oligomers leads to further growth of polymeric precursors in the CH_3SO_3H-catalyzed system.

Keywords 2D GPC correlation · Aggregate · Triethoxysilyl-terminated polystyrene · Reactivity · Trimer · Nature of catalyst

Introduction

Suzuki et al. [1] have previously reported details of the acid-catalyzed condensation reaction of five well-defined polymeric silane coupling agents (SCAs), triethoxysilyl-terminated polystyrenes (TESi-PS), substituted with various polystyrene portions of high molecular weight. The results showed that the degree of polycondensation depends on the nature of both catalyst and solvent used in the reaction. Suzuki et al. [2] presented further data on the combined effects of the amount of polystyrene included and the use of non-polar solvents on the reaction rate of high molecular weight TESi-PS. They provided irrefutable evidence for the formation of aggregates which accelerate the reaction rate during the polycondensation. Further support for such an aggregational model has been reported [3, 4, 5]. Ogasawara et al. [6] and Izawa et al. [7] used time-resolved small-angle X-ray scattering spectra to detect the aggregates of relatively simple SCAs in ethanol.

Izawa et al. [8, 9, 10] were the first to introduce the 2D GPC correlation method to investigate intricate details of the polycondensation of a relatively simple SCA, perfluoro-octyltriethoxysilane, catalyzed by 1 mol/l HCl. The results indicated that the mechanism of the growth process of the polycondensed aggregates is strongly reflected in the patterns of the 2D GPC correlation spectra. Furthermore, the 2D GPC correlation spectra of the same SCA sample [11] demonstrated a splitting of the elution band, which consists of two (reactive and much less reactive) components, leading to the conclusion that these reactive components induce rapid growth of polycondensed aggregates.

In our previous paper [11], gel-permeation chromatography (GPC) profiles were collected as a function of reaction time for the two-step polycondensation of two TESi-PS molecules, with molecular weights equal to 2400 and 8000, catalyzed by CH_3SO_3H in THF. The two sets of the time-resolved GPC profiles were then converted into two-dimensional (2D) GPC correlation spectra [8, 9, 10] based on the generalized 2D correlation theory [12]. The 2D GPC correlation spectra thus obtained provided details of the aggregate-aggregate correlations, which reflect the effect of aggregation on the polycondensation. In particular, splitting of elution bands in the 2D GPC correlation spectra was found, and its origin was discussed in relation to the reaction mechanism.

In this study, a set of time-resolved GPC profiles, collected from the reaction mixture of the HCl-catalyzed TESi-PS-THF system, was used to calculate the 2D GPC correlation spectra. In particular, the effect of HCl as a catalyst on the growth of polycondensed precursors is discussed by comparing the results with those of the CH_3SO_3H- catalyzed TESi-PS system [11].

Experimental

Materials Living polystyrene (PS) with molecular weight (Mn) equal to 7800 was synthesized by anionic polymerization of styrene [1, 2, 13]. Triethoxysilyl-terminated polystyrenes (TESi-PS) with Mn equal to 8000 was prepared by the coupling reaction of living PS and chlorotriethoxysilane [13]. The sample (TESi-PS (8000)) thus obtained was recrystallized in methanol, and after drying in vacuum at ca. 298 K, was used for condensation. Samples of the two reaction systems were placed into ampoules. System I consists of TESi-PS (8000) (40 mmol/kg), catalyst (HCl, 0.1 mol/kg) and tetrahydrofuran (THF), while System II is made of TESi-PS (8000) (40 mmol/kg), catalyst (CH_3SO_3H, 0.1 mol/kg) and THF., The mixtures were sealed under high vacuum (10^{-3} mm Hg) and homogenized by shaking. Condensation of TESi-PS (8000) in each reaction mixture was carried out in a temperature-controlled bath (333 K) for a prescribed time. The condensed products of TESi-PS (8000), precipitated from each reaction mixture, were filtered through a glass filter and dried at ca. 298 K.

The yield value Y (%) of polycondensed TESi-PS (8000) was calculated from the GPC curve of the recovered polymer using the equation

$$Y = 100\% \times (\text{GPC peak area of polymerized TESi} - \text{PS}(8000))/(\text{total GPC peak area of the reacted products}). \quad (1)$$

The functionality of TESi-PS (8000) (f (%), defined as the maximum Y value of TESi-PS (8000)), was 98%. The contribution of the band for the unfunctionalized trace constituent to the band for the total condensed product was 2%. This contribution was subtracted from the area of polycondensed TESi-PS to obtain the value of Y.

Time-resolved GPC measurements A GPC calibration curve with linear PS standards [11] was used to determine the degree of polycondensation of the condensed TESi-PS polymers, since it has already been confirmed that this technique can be applied to the branched products of TESi-PS [14]. A Toso HLC-802A (with two GMH columns), equipped with a refractive index (RI) detector (column oven temperature 313 K) was used for the GPC measurements. The nominal flow rate of the eluent (THF) was 1 mL/min. The actual flow rates were inspected during the recording of a GPC curve, and their constancy was confirmed (the errors of an elution count; ± 0.1 min). The average signal-to-noise ratio of the GPC data was less than 170.

2D GPC correlation analysis Synchronous and asynchronous 2D GPC correlation spectra were calculated from the time-resolved GPC profiles (using the 2D OGAIZA software developed at Nagoya Institute of Technology). The theoretical background of the 2D GPC spectra is described in recent publications [8, 9, 10].

Results

Time resolved GPC profiles

Time dependent GPC profiles ($t = 0$, 1, 4, 24, 768 h) of the TESi-PS (8000)-THF system catalyzed by HCl (0.1 mol/kg) (System I) are shown in Fig. 1A. Assignments of the elution bands, made on the basis of the PS-standard calibration curve [11], are listed in Table 1 together with those based on the 2D GPC correlation spectra. The time-resolved GPC profiles thus measured provide information on the time-dependence of the composition of the reaction system. A predominant elution band at 33.9 min (band A) appears at reaction

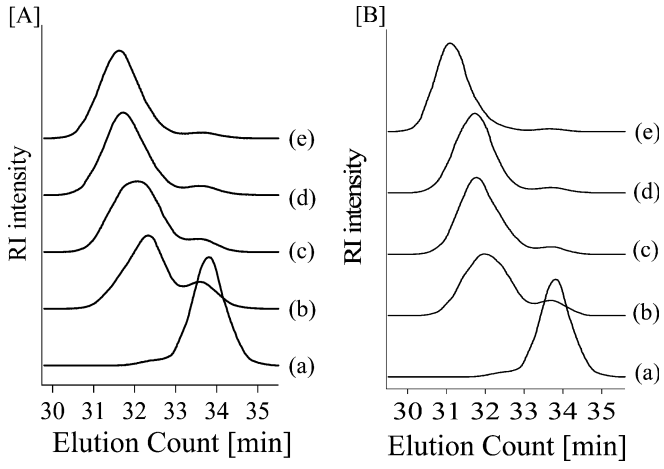

Fig. 1A,B Time-resolved GPC elution profiles of: **A** the HCl (0.1 mol/kg) -catalyzed TESi-PS (8000)-THF system; **B** the CH_3SO_3H (0.1 mol/kg) -catalyzed TESi-PS (8000)-THF system. Times: (a), 0 h; (b), 1 h; (c), 4 h; (d), 24 h; (e), 768 h

Table 1 Tentative assignment of elution peaks[a]

Conventional GPC		2D GPC		Assignment[c]
Counts (min)	Band no.	Counts (min)	Band no.[b]	
		34.0–34.2	A_H	Hydrolyzed and partially hydrolyzed monomer
33.8	A	33.7–33.9	A	TESi-PS (monomer) and partially hydrolyzed monomer
		33.3–33.5	A_L	Solvated monomer
		32.8	B_H	Hydrolyzed dimer
32.5	B	32.4–32.5	B	Dimer
		32.1–32.2	B_L	Solvated dimer
31.6	C	31.6–31.8	C	Trimer
		31.4	C_L	
31.0	D	31.1	D	Tetramer
		30.8	E	Pentamer
		30.6	E′	

[a]The errors of elution count are ±0.1 min
[b]Subscript H = high elution component; subscript L = low elution component
[c][8, 11]

time t = 0 h, and is assigned to the TESi-PS monomers. With elapse of time, an elution band emanating from the oligomeric species appears at lower elution count, and as its intensity increases, this band shifts to even lower elution count, while the intensity of the monomeric band (A) is seen to decrease more rapidly. This observation indicates that consumption of the TESi-PS (8000) monomers is accompanied by formation of clusters which increase in size, and consequently, the fractions of the oligomeric species change with reaction time.

To examine the effect of a different catalyst on the polycondensation, the GPC profiles of the CH_3SO_3H-catalyzed TESi-PS-THF system (System II) were also measured over a long time scale (Step I: 0, 1, 4 h, and Step II: 4, 24, 768 h). Time dependent GPC profiles of System II are shown in Fig. 1B. Assignments of the elution bands are listed in Table 1. When we compare the time-resolved GPC profiles of the two systems, we find that System I apparently furnishes trimers as final products, while System II brings about tetramers. This fact implies that the nature of the catalyst affects the growth process of the polymeric precursor.

In order to understand details of the difference in reaction mechanism between these two systems, we have examined the process of polycondensation in System I, using the 2D GPC correlation technique, which made it possible to elucidate details of the polycondensation reactions [8, 9, 10, 11]. We were then able to compare these 2D GPC correlation spectra with those of System II [11]. Based on the time dependence of the Y value, we could assume that the polycondensation of these two systems consists of two steps (I (t = 0, 1 and 4 h) and II (t = 4, 24 and 768 h)).

2D GPC correlation spectra of System I

The synchronous and asynchronous 2D GPC correlation spectra of System I were calculated from a set of time-resolved GPC profiles and are shown in Figs. 2 and 3, respectively. The possible synchronous correlation squares (CSqi, where i = 1–3) and their corresponding band correlations are listed in Table 2 together with the coordinates. Band correlations, signs and order of events are listed in Table 3.

In the synchronous map (step I) of System I (Fig. 2A), the correlation square CSq_1 appears and is constructed from two autopeaks and two cross peaks. According to the 2D correlation theory [12], the following facts may be directly derived from these correlations:

1. The TESi-PS (8000) monomers (band A) are rapidly consumed to form a dimer (band B, and in particular, component B_L), providing two autopeaks (Table 2). A very strong autopeak (33.9, 33.9) is extended in the region from 33.0 to 34.7 min, implying that dynamic variation of component A is predominant. In other words, of the three components A_L, A and A_H produced in the early stage (0–1 h), most of the A_L and A_H components have already been consumed in step I. The autopeak coming from band B is also extended in the region from 31.0 to 33.0 min. The components (B_L, B and B_H) of band B and the components (C_L and C) of band C, produced in the early stage, are included in this region. However, production of component B_L contributes mainly to step I.

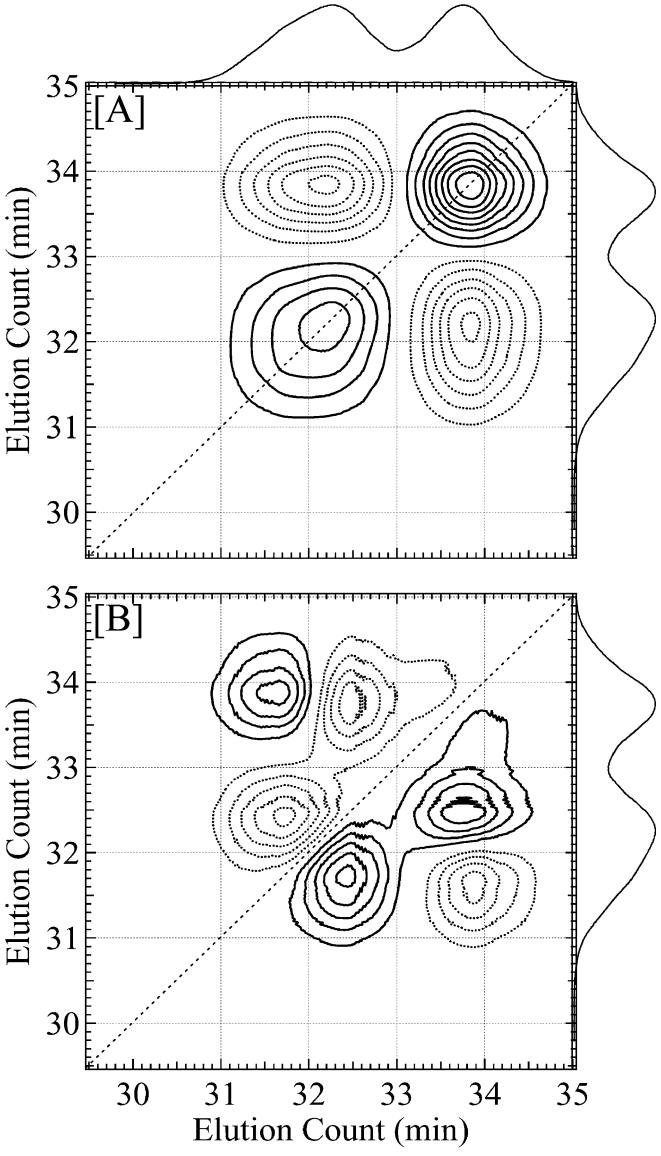

Fig. 2A Synchronous spectra. **B** Asynchronous spectra of step I (0, 1, 4 h) for the HCl-catalyzed TESi-PS (8000)-THF system

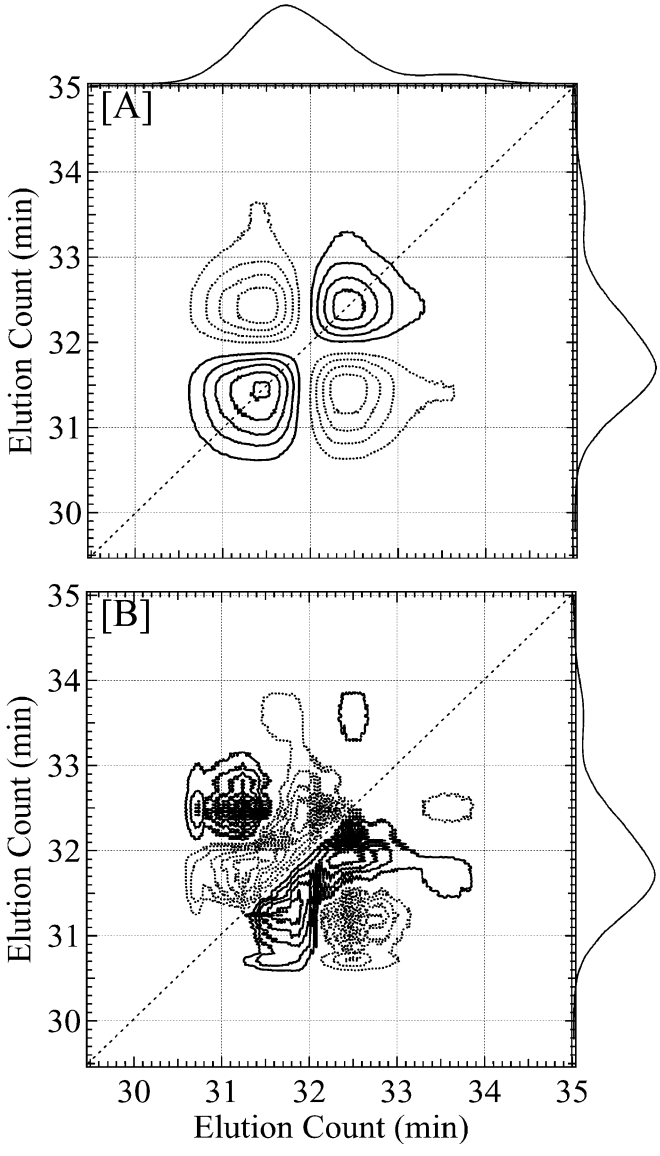

Fig. 3A Synchronous spectra. **B** Asynchronous spectra of step II (4, 24, 768 h) for the HCl-catalyzed TESi-PS (8000)-THF system

2. A coordinated decrease in intensity of band A and simultaneous increase in that of band B_L occurs, providing two negative cross peaks (A↔B_L), thus implying that formation of component B_L is a consequence of the consumption of component A.
3. Dynamic variation in concentration of the monomers (probably via hydrolysis) of TESi-PS (8000) makes a major contribution to step I. That is, the presence of square CSq_1 implies that coherent variation in intensities of bands A and B_L exists at the time of their elution.

In the synchronous maps (step II, Fig. 3A), square CSq_1 is constructed. However, very weak correlation squares, CSq_2 and CSq_3, are also present. These correlations provide the following information.

4. The dimers (band B) are consumed to produce the trimer (band C), providing two relatively strong autopeaks and a very weak autopeak.
5. There is a coordinated decrease in intensity of band B and simultaneous increase in intensity of band C, providing negative cross peaks (B↔C).
6. (The B↔C correlation contributes mainly to step II.) The A↔C correlation is very weak.

In the asynchronous maps (step I) of System I, (Fig. 2B), the resolution enhancing characteristics of the 2D GPC spectra [12] provide further details of the band

Table 2 Possible correlation squares (CSq_i) and correlations[a] between the elution peaks in steps I and II for the HCl-catalyzed TESi-PS (8000)-THF system

[a]vs: very strong, s: strong, m: medium, w: weak, vw: very weak
[b]Very weak

CSq_i	Coodinates (E_1, E_2)				Correlation	
	Autopeak		Cross-peak			
Step I (0–4 h)						
CSq_1	$+(33.9, 33.9)_{vs}$	$+(32.2, 32.2)_{m}$	$-(33.9, 32.2)_{s}$	$-(32.2, 33.9)_{s}$	A	B_L
Step II (4–768 h)						
CSq_1	$+(32.4, 32.4)_{m}$	$+(31.4, 31,4)_{s}$	$-(32.4, 31.4)_{m}$	$-(31.4, 32.4)_{m}$	B	C
(CSq_2)[b]	$+(33.3, 33.3)_{vw}$	$+(32.4, 32.4)_{vw}$	$+(33.3, 32.4)_{vw}$	$+(32.4, 33.3)_{vw}$	A_L	B
(CSq_3)[b]	$+(33.3, 33.3)_{vw}$	$+(31.4, 31.4)_{vw}$	$-(33.3, 31.4)_{vw}$	$-(31.4, 33.3)_{vw}$	A_L	C

correlations in the polycondensation process. Medium A↔C and strong B↔C correlations exist, in addition to a medium A↔B correlation. That is, component A correlates with component B, providing the positive cross peak at (33.8, 32.4) min, but it also correlates with component C, resulting in the negative cross peak at (33.9, 31.6) min. The appearance of the positive cross peak at (32.4, 31.7) min indicates the existence of a B↔C correlation, with the dimer (band B) changing first followed by the trimer (band C). We note that component C, in addition to component B, is produced rapidly in step I.

In the asynchronous spectrum (step II) of System I (Fig. 3B), we find that band B consists of components B_H, B and B_L, providing the weak positive cross peak at (32.8, 32.2) and the very strong positive cross peak at (32.5, 32.2) min. Correlation of the B_H component with that of C_L yields the medium negative fused cross peak at (32.8, 31.2) min. The positive cross peak at (32.5, 31.9) min arises from the B↔C correlation, while the very strong negative fused-type cross peak at (32.5, 30.8–31.5) min comes from the strong correlation of component B with the C_L and D components. The weak negative cross peak at (32.2–32.9, 30.7) may be assigned to the correlations of band E with the B_H, B and B_L components. However, the correlation of component B_H with those of C_L, D and E are not as strong as those of the B component. The appearance of the strong positive cross peak at (31.8, 31.3) min indicates directly that band C consists of components C (31.8 min) and C_L (31.2–31.3 min). The positive cross peak at (31.3–31.9, 30.7) min is assigned to the correlation of the C component with band E. However, it should be emphasized that component C_L does not correlate with any other bands in step II.

2D GPC correlation spectra of System II.

In order to compare the synchronous and asynchronous behaviors for System I with those for System II [11], the 2D GPC correlation spectra of the CH_3SO_3H-catalyzed system were re-calculated from a set of time-resolved GPC profiles, which included the GPC profile measured after 768 h for the same sample (spectrum not shown). The possible synchronous correlation square (CSq_i) and the corresponding band correlations are listed in Table 4. Synchronous and asynchronous band correlations, signs and order of events are listed in Table 5.

Table 3 Synchronous and asynchronous peak correlations, signs and order of events for the HCl-catalyzed TESi-PS (8000)-THF system

[a]vs: very strong, s: strong, m: medium, w: weak, vw: very weak
[b]Synchronous
[c]Asynchronous
[d]$E_x \rightarrow E_y$; the event E_x occurs before E_y
[e]Subscripts H and L represent, respectively, high and elution components

Step	Correlation[a]				Sign		Order of events[d,e]		
					(Φ)[b]	(Ψ)[c]			
I	A	↔	A_L	(vw)	+	+	A	→	A_L
	A	↔	B	(m)	−	+	B	→	A
	A	↔	B_L	(m)	+	+	A	→	B_L
	A	↔	C	(m)	−	-	A	→	C
	B	↔	C	(s)	+	+	B	→	C
II	A	↔	B	(vw)	+	−	B	→	A
	A	↔	C	(vw)	−	+	C	→	A
	B_H	↔	B_L	(vw)	+	+	B_H	→	B_L
	B_H	↔	C_L,D,E	(w)	+	−	C_L,D,E	→	B_H
	B	↔	B_L	(vs)	+	−	B_L	→	B
	B	↔	C	(m)	+	+	B	→	C
	B	↔	C_L,D	(vs)	+	−	C_L,D	→	B
	B	↔	E	(w)	+	−	E	→	B
	B_L	↔	C_L,D	(m)	−	−	B_L	→	C_L,D
	C	↔	C_L	(s)	+	+	C	→	C_L
	C	↔	D	(m)	+	+	C	→	D
	C	↔	E	(w)	+	+	C	→	E

Table 4 Possible correlation squares (CSqi) and correlations[a] between the elution peaks in steps I and II for the CH_3SO_3H-catalyzed TESi-PS (8000)-THF system

[a] vs: very strong, s: strong, m: medium

CSq_i	Coodinates (E_1, E_2)				Correlation	
	Autopeak		Cross-peak			
Step I (0–4 h)						
CSq_1	$+(33.8, 33.8)_s$	$+(31.8, 31.8)_m$	$-(33.8, 31.8)_m$	$-(31,8, 33,8)_m$	A	C
Step II (4–768 h)						
CSq_1	$+(31.9, 31.9)_m$	$+(31.0, 31.0)_{vs}$	$-(31.9, 31.0)_s$	$-(31,0, 31,9)_s$	C	D

The synchronous and asynchronous maps for System II (Table 5) provide the following results:

1. The A↔C correlation square (CSq_1) in step I reflects occurrence of coherent variation of GPC intensities at these elution times, implying that hydrolysis of the TESi-PS (8000) monomers (band A) occurs rapidly to form the trimer (band C).
2. In step II, coherent variation in the intensities of bands C and D occurs, providing the C↔D correlation square which implies consumption of the trimer (band C) to produce the tetramer (band D).

The notable results obtained from resolution enhancement of the asynchronous maps of the two systems, may be summarized as follows.

Table 5 Synchronous and asynchronous peak correlations, signs and order of events for the CH_3SO_3H-catalyzed TESi-PS (8000)-THF system

Step	Correlation[a]				Sign		Order of events[d,e]		
					(Φ)[b]	(Ψ)[c]			
I	A	↔	A_L	(vw)	+	+	A	→	A_L
	A	↔	B	(s)	+	+	A	→	B
	A	↔	C	(vs)	−	-	A	→	C
	A	↔	C_L	(m)	−	-	A	→	C_L
	A	↔	D,E	(vw)	−	-	A	→	D,E
	B_H	↔	C,C_L	(w)	+	+	B_H	→	C,C_L
	B,B_L	↔	C	(vs)	+	+	B,B_L	→	C
	B,B_L	↔	C_L	(m)	+	+	B,B_L	→	C_L
	B,B_L	↔	D	(vw)	+	+	B,B_L	→	D
II	B_H,B	↔	C	(m)	+	+	B_H,B	→	C
	B_H,B	↔	D	(m)	−	-	B_H,B	→	D
	B_H,B	↔	E	(m)	−	-	B_H,B	→	E
	B_H,B	↔	E′	(w)	−	-	B_H,B	→	E’
	C	↔	C_L	(m)	+	+	C	→	C_L
	C	↔	D	(m)	+	+	C	→	D
	C_L	↔	D	(m)	+	+	C_L	→	D
	C_L	↔	E	(m)	+	+	C_L	→	E
	C_L	↔	E′	(w)	+	+	C_L	→	E’
	D	↔	E,E′	(w)	+	+	D	→	E,E’

[a] vs: very strong, s: strong, m: medium, w: weak, vw: very weak
[b] Synchronous
[c] Asynchronous
[d] $E_x \rightarrow E_y$; the event E_x occurs before E_y
[e] Subscripts H and L represent, respectively, high and low elution components

The relatively strong correlations of components B and B_L with component C and C_L, as well as the strong correlations of band A with components B, C and C_L, appear in step I.

Although the A↔B and A↔C correlations do not appear in step II, medium correlations of components B_H and B with C, D and E, and medium C↔C_L, C↔D and C_L↔E correlations do appear. Components C_L and D further correlate weakly with E or E′.

Discussion

Analysis of the time-resolved GPC profiles of the two reaction systems (I and II) yielded the result that the trimer in System I and the tetramer in System II were preferentially stabilized after 768 h. Differences in the reaction mechanism of the two systems is better elucidated by using the 2D GPC correlation technique.

The 2D GPC correlation spectra represent directly the reaction or interaction mechanism during the polycondensation. In Schemes I (System I) and II (System II), the possible sequence of these intricate reactions or interactions can be discussed by assuming the following cascade steps.

[Scheme I]
Step I

$$2\,A \underset{\leftarrow}{\rightarrow} B \text{ or } B_L \quad (1)$$

$$B + A \underset{\leftarrow}{\rightarrow} C \quad (2)$$

$$3A \underset{\leftarrow}{\rightarrow} C \quad (3)$$

Thus, the trimer finally becomes the predominant product in step I. Since the monomers may form an aggregate [2], step (3) may also be possible.

Step II

$$B + A \underset{\leftarrow}{\rightarrow} C \quad (4)$$

$$C + A \underset{\leftarrow}{\rightarrow} D \quad (4')$$

$$2B_L,\ 2B \underset{\leftarrow}{\rightarrow} D \quad (5)$$

$$2B_H \underset{\leftarrow}{\rightarrow} D \quad (6)$$

$$\left.\begin{array}{l} B_L + A \underset{\leftarrow}{\rightarrow} C_L \\ B + A \underset{\leftarrow}{\rightarrow} C_L \\ B_H + (A) * \underset{\leftarrow}{\rightarrow} C_L \end{array}\right\} \quad (7)$$

where $(A)^*$ represents components A_L or A or A_H.

Steps (4) and (7) occur preferentially, resulting in predominant production of the trimer (C and C_L). In particular, it should be noted that correlation of component C_L with a longer oligomer does not exist, implying that the C_L component does not lead to growth of longer oligomers. Accordingly, we may assume that component C_L is much less reactive, compared with component C. Since components B_L, B and B_H are consumed to form the C_L species (cascade steps (7)), the contribution of the D species formed in cascade steps (5) and (6) to the whole process in step II becomes small. Thus, instead of the production of component D, the trimers (C and C_L) are preferentially stabilized. Although there may exist other reaction routes (e.g., A↔B, A↔C, B or B_H or C↔E) during step II, their total contribution to the whole process must be small.

[Scheme II]
Step I

$$2A \underset{\leftarrow}{\rightarrow} B \quad (1)$$

$$\left.\begin{array}{l} B + (A) * \underset{\leftarrow}{\rightarrow} C \\ B_L + (A) * \underset{\leftarrow}{\rightarrow} C \end{array}\right\} \quad (2)$$

$$3A \underset{\leftarrow}{\rightarrow} C \quad (3)$$

$$\left.\begin{array}{ll} 3A & \underset{\leftarrow}{\rightarrow} C_L \\ B_L + (A)* & \underset{\leftarrow}{\rightarrow} C_L \\ B_H + (A)* & \underset{\leftarrow}{\rightarrow} C_L \end{array}\right\} \quad (4)$$

where $(A)^*$ represents A_L or A or A_H components.

Steps (2) - (4) contribute to predominant production of the trimer (C and C_L) in this step. The contribution of other reaction routes (e.g. B_H) ↔ C or C_L, B_L or B ↔ D, and A ↔ E) to the whole process (step I) must be small.

Step II

$$\left.\begin{array}{ll} B + (A)* & \underset{\leftarrow}{\rightarrow} C \\ B_H + (A)* & \underset{\leftarrow}{\rightarrow} C \end{array}\right\} \quad (5)$$

$$\left.\begin{array}{l} 2B \underset{\leftarrow}{\rightarrow} D \\ 2B_H \underset{\leftarrow}{\rightarrow} D \end{array}\right\} \quad (6)$$

$$C + (A) * \underset{\leftarrow}{\rightarrow} D \quad (7)$$

$$C_L + (A) * \underset{\leftarrow}{\rightarrow} D \quad (7')$$

$$\left.\begin{array}{l} B + (C) * \underset{\leftarrow}{\rightarrow} E \\ 2B + (A) * \underset{\leftarrow}{\rightarrow} E \end{array}\right\} \quad (8)$$

$$\left.\begin{array}{l} B_H + (C) * \underset{\leftarrow}{\rightarrow} E \\ 2B_H + (A) * \underset{\leftarrow}{\rightarrow} E \end{array}\right\} \quad (9)$$

$$\left.\begin{array}{l} C_L + (B) * \underset{\leftarrow}{\rightarrow} E \\ C_L + (2A) * \underset{\leftarrow}{\rightarrow} E \end{array}\right\} \quad (10)$$

where $(B)^*$ represents components B_L or B or B_H, and $(C)^*$ represents components C or C_L.

The contribution of other routes (e.g., D↔E or E′, C_L↔E′) to step II (Scheme II) is small. The parallel occurrence of reaction routes, steps (5), (6) and (7') probably results in preferential production of the tetramer (D) in step II. In particular, steps (7') and (10) indicate that the C_L species reacts with monomeric or dimeric species to form the tetramer or the pentamer. Therefore, the C_L component in System II is responsible for elongation of the precursors. Furthermore, from the existence of the relatively strong correlations, B_H, B↔E and C_L↔E, we may assume that formation of pentamer occurs in step II through steps (8), (9) and (10), albeit to a relatively small extent, indicating that these reactive components participate in formation of the pentamer.

The reason why trimer and tetramer are preferentially stabilized after 768 h in both the HCl- and CH_3SO_3H-catalyzed systems, respectively, may be ascribed to the difference in reactivity of the trimeric species (C and C_L). Although they are common to both systems, only component C is reactive in both, while component C_L is unreactive in System I and reactive in System II. We may now stress that the species of catalyst used for the condensation affects the reactivity of the trimeric species. Further research on the effect of different catalytic species on the polycondensation and on the natures of the trimeric species is highly desirable.

In our previous study [11], we suggested that formation of a TESi-PS oligomer with high reactivity may play a critical role in the elongation process, although a hydrophobic interaction (that is, aggregation) between oligomers should hinder elongation of a polymer via Si-O-Si bond formation. In particular, reactivity of oligomers may be intrinsically correlated with their steric structures. For example, Takaki et al. [15] reported that the final product for the HCl-catalyzed TESi-PS-THF system was the trimer which underwent little or no hydrolysis, indicating low reactivity.

It is possible that the differing reactivity of the trimers arises from the presence of differing polycondensation structures for these trimers. Some evidence is

available to support the presence of cyclic structures but the exact nature of such cyclic products is not able to be determined from the results described herein. However, we do know that the silicic acid monomer ($Si(OH)_4$) has a strong tendency to form cyclic structures during the early polycondensation process [16], and that TESi-PS molecules may form cyclic trimers in the polar core of reversed micellar type aggregates [2]. The exact nature of the different species awaits investigation by another technique, such as ^{29}Si-NMR.

The appearance of reactive and less-reactive trimers (bands C and C_L) probably arises from the condensation reaction within the TESi-PS aggregates in THF. Based on the results of the SAXS [7], ^{1}H NMR [6] and 2D NIR [17] studies of the HCl-catalyzed PFOTES-ethanol system their origin may be accounted for as follows. In step I, hydrolysis of the ethoxy groups commences, and consequently, mono-, di- and tri-hydrolysis of monomers results in production of small oligomers (dimers and trimers) with ethoxy groups remaining unreacted [6]. A marked steric hindrance of the bulky and highly rigid PS chains may promote stabilization of ethoxy groups, which contributes to the self-assembly of the PS chains [2, 7]. In step II, condensation between small clusters is predominant, leading to further growth of small clusters with unreacted ethoxy groups and release of many silanols. The silanol groups thus produced may be stabilized by interaction with water, ethanol and silanol itself through hydrogen bonding, to form a weakly or strongly associated self-assembly of SiOH groups [7, 17].

A kinetic model, which explains the growth processes of polycondensation and aggregation that occur far from equilibrium, has been presented by Witten et al. [18], Sander [19], Schaefer [20], and Daoud et al. [21] for the growth process of silica polymers. Schaefer [20] described the kinetic model of monomer-cluster (MC) growth and cluster-cluster (CC) growth. The MC and CC growth models correspond to the two growth processes, steps I and II, respectively, of the polycondensed precursors in the two systems, as evidenced by formation of small oligomers in step I and larger oligomers in step II.

In our previous paper [1], we evaluated the activity of various acid catalysts in the TESi-PS-THF system. We showed that there were no correlations between the catalytic activities and pKa values of acid catalysts. The observation leads to the conclusion that the catalytic activity of an acid may not only be related to the characteristics as a proton donor but also to other possible effects, for example, the manner of coordination of its counter anion (Cl^- or $CH_3SO_3^-$) to the polar moieties of TESi-PS.

Conclusion

The 2D GPC correlation technique has been used to examine the difference in the polycondensation mechanism of TESi-PS (8000), catalyzed by two catalytic species. It has been found that the nature of the catalyst affects the mechanism of TESi-PS polycondensation. In System I, catalyzed by HCl, predominant production of a less-reactive trimer occurs, hindering the further growth of trimer. Conversely, in System II, catalyzed by CH_3SO_3H, formation of a reactive trimeric species occurs, leading to further growth of the precursors.

References

1. Suzuki K, Esaki M, Misawa A, Takaki M (1994) Kobunshi Ronbunshu 51:11
2. Suzuki K, Oku J, Okabayashi H, O'Connor CJ (2003) Langmuir 19:7611
3. Munir A, Goethals EJ (1981) Makromol Chem Rapid Commun 2:693
4. Lee KW, MacCarthy TJ (1988) Macromolecules 21:3353
5. Chujo Y, Ihara E, Ihara H, Saegusa T (1989) Macromolecules 22:2040
6. Ogasawara T, Izawa K, Hattori N, Okabayashi H, O'Connor CJ (2000) Colloid Polym Sci 278:293
7. Izawa K, Ogasawara T, Masuda H, Okabayashi H, Monkenbnsch M, O'Connor CJ (2002) Colloid Polym Sci 280:725
8. Izawa K, Ogasawara T, Masuda H, Okabayashi H, Noda I (2002) Macromolecules 35:92
9. Izawa K, Ogasawara T, Masuda H, Okabayashi H, O'Connor CJ, Noda I (2002) J Phys Chem B 106:2867
10. Izawa K, Ogasawara T, Masuda H, Okabayashi H, O'Connor CJ, Noda I (2002) Phys Chem Chem Phys 4:1053
11. Suzuki K, Oku J, Izawa K, Okabayashi H, Noda I, O'Connor CJ (2004) Colloid Polym Sci (in press)
12. Noda I (1993) Appl Spectrosc 47:1329
13. Suzuki K, Oku J, Okabayashi H, O'Connor CJ (2003) Polym J 35:938
14. Suzuki K, Katsumura G, Kondo Y, Oku J, Takaki M (1992) Kobunshi Ronbunshu 49:825
15. Takaki M, Suzuki K, Kondo Y, Oku J (1991) Polym J 23:917
16. Iler RK (1979) The chemistry of silica—solubility, polymerization, colloid and surface properties and biochemistry. Wiley, New York, p 175
17. Izawa K, Ogasawara T, Masuda H, Okabayashi H, O'Connor CJ (2002) Colloid Polym Sci 280:380
18. Witten TA, Cates ME (1986) Science 232:1607
19. Sander LM (1987) Sci Am 256:94
20. Schaefer DW (1989) Science 243:94
21. Daoud M, Martin JE (1989) In: Avenir D (ed) The fractal approach to heterogeneous chemistry. Wiley, New York, p 109